JOC Article

Kinetic Stabilities of Double, Tetra-, and Hexarosette Hydrogen-Bonded Assemblies

Leonard J. Prins, Edda E. Neuteboom, Vasile Paraschiv, Mercedes Crego-Calama, Peter Timmerman,* and David N. Reinhoudt*

Laboratory of Supramolecular Chemistry and Technology, MESA Research Institute, University of Twente, P.O. Box 217, 7500 AE Enschede (The Netherlands)

d.n.reinhoudt@ct.utwente.nl

Received February 12, 2002

A study of the kinetic stabilities of hydrogen-bonded double, tetra-, and hexarosette assemblies, comprising 36, 72, and 108 hydrogen bonds, respectively, is described. The kinetic stabilities are measured using both chiral amplification and racemization experiments. The chiral amplification studies show that solvent polarity and temperature strongly affect the kinetic stabilities of these hydrogen-bonded assemblies. For example, the activation energy for the dissociation of a tetramelamine from a tetrarosette assembly, a process that involves the breakage of 24 hydrogen bonds, was determined at 98.7 ± 16.6 kJ mol^{-1} in chloroform and 172.8 ± 11.3 kJ mol^{-1} in benzene. Moreover, racemization studies with enantiomerically enriched assemblies reveal a strong dependence of the kinetic stability on the number and strength of the hydrogen bonds involved in assembly formation. The half-lives for double, tetra-, and hexarosette assemblies were found to be 8.4 min, 5.5 h, and 150 h in chloroform at 50 °C, respectively. For higher generations of these types of assemblies, the kinetic stabilities become so high that they can no longer measured in a direct manner.

Introduction

One of the most attractive features of noncovalent assemblies is their clean and quantitative formation, which is due to their ability to display error-correction.[1−4] This implies that any structural "mistake" in the assembly is corrected automatically, the result of the fact that 'mismatched' assemblies are generally much higher in energy. The only prerequisite for error-correction to occur is that the activation energy for interconversion of 'mismatched' structures is lower than the thermal energy present in the system. In virtually all noncovalent assemblies reported to date this is the case, since only few weak interactions have to be broken in order to disassemble. However, there are several exceptions. For assemblies based on strong metal−ligand interactions, such as Fe^{II}-bipyridine[5] or Pt^{II}-pyridine,[6,6] initial formation of a large number of kinetic products has been observed. In these cases the activation energy is so high that interconversion to the thermodynamic products occurs only after extensive heating. For hydrogen-bonded assemblies, similar phenomena were first reported by Whitesides in double[7] and triple rosette[8] assemblies that are held together by 36 and 48 H-bonds, respectively. Also in these cases complete conversion to the thermodynamic products was observed within hours. Recently, we observed the formation of highly stable kinetic products in the formation of tetrarosette assemblies.[9] In light of these observations we studied a variety of hydrogen-bonded assemblies with respect to their kinetic stabilities in solution.

This paper describes hydrogen-bonded rosette assemblies displaying kinetic stabilities comparable to those of assemblies based on metal−ligand coordinative interactions or even covalent molecules. The study is a follow-up of our investigations on the remarkably high kinetic stability observed for double rosette assemblies $\mathbf{1}_3\cdot(CA)_6$,[10,11] and includes tetrarosette assembly $\mathbf{2}_3\cdot(CA)_{12}$ and hexarosette assembly $\mathbf{3}_3\cdot(CA)_{18}$ (Figure 1).[12,13] Kinetic

* To whom correspondence should be addressed. Fax: (+31)-53-4894645.

(1) Lindsey, J. S. *New J. Chem.* **1991**, *15*, 153−180.
(2) Whitesides, G. M.; Simanek, E. E.; Mathias, J. P.; Seto, C. T.; Chin, D. N.; Mammen, M.; Gordon, D. M. *Acc. Chem. Res.* **1995**, *28*, 37−44.
(3) Philp, D.; Stoddart, J. F. *Angew. Chem.* **1996**, *108*, 1242−1286; *Angew. Chem., Int. Ed. Engl.* **1996**, *35*, 1154−1194.
(4) Prins, L. J.; Reinhoudt, D. N.; Timmerman, P. *Angew. Chem.* **2001**, *113*, 2446−2492; *Angew. Chem., Int. Ed.* **2001**, *40*, 2383−2426.
(5) Hasenkopf, B.; Lehn, J.-M.; Boumediene, N.; Leize, E.; Van Dorsselaer, A. *Angew. Chem.* **1998**, *110*, 3458−3460; *Angew. Chem., Int. Ed.* **1998**, *37*, 3265−3268.
(6) Fujita, M.; Ibukuro, F.; Yamaguchi, K.; Ogura, K. *J. Am. Chem. Soc.* **1995**, *117*, 4175−4176.
(7) Mathias, J. P.; Seto, C. T.; Simanek, E. E.; Whitesides, G. M. *J. Am. Chem. Soc.* **1994**, *116*, 1725−1736.
(8) Mathias, J. P.; Simanek, E. E.; Seto, C. T.; Whitesides, G. M. *Angew. Chem.* **1993**, *105*, 1848−1852; *Angew. Chem., Int. Ed. Engl.* **1993**, *32*, 1766−1769.
(9) Paraschiv, V.; Fokkens, R. H.; Padberg, C. J.; Timmerman, P.; Reinhoudt, D. N. *J. Org. Chem.* **2001**, *66*, 8297−8301.
(10) Prins, L. J.; De Jong, F.; Timmerman, P.; Reinhoudt, D. N. *Nature* **2000**, *408*, 181−184.
(11) Prins, L. J.; Verhage, J.; De Jong, F.; Timmerman, P.; Reinhoudt, D. N. *Chem. Eur. J.* **2002**, *8*, 2302−2313.
(12) Jolliffe, K. A.; Timmerman, P.; Reinhoudt, D. N. *Angew. Chem.* **1999**, *111*, 983−986; *Angew. Chem., Int. Ed.* **1999**, *38*, 933−937.
(13) Paraschiv, V.; Crego-Calama, M.; Ishi-i, T.; Padberg, C. J.; Timmerman, P.; Reinhoudt, D. N. *J. Am. Chem. Soc.*, in press.

10.1021/jo0201023 CCC: $22.00
Published on Web 06/18/2002

CHART 1

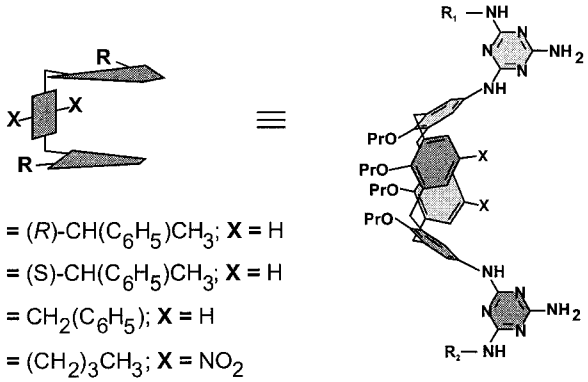

1a $R_1 = R_2 = (R)\text{-}CH(C_6H_5)CH_3$; **X** = H

1b $R_1 = R_2 = (S)\text{-}CH(C_6H_5)CH_3$; **X** = H

1c $R_1 = R_2 = CH_2(C_6H_5)$; **X** = H

1d $R_1 = R_2 = (CH_2)_3CH_3$; **X** = NO_2

1e $R_1 = CH_2CH(CH_3)_2CH_2NH_2$
$R_2 = CH_2CH(CH_3)_2CH_2NH$ -Boc; **X** = H

1f $R_1 = CH_2CH(CH_3)_2CH_2NH_2$
$R_2 = CH_2CH(CH_3)_2CH_2NHCONH(CH_2)_4$-
-$NHCOOpNO_2Ph$; **X** = H

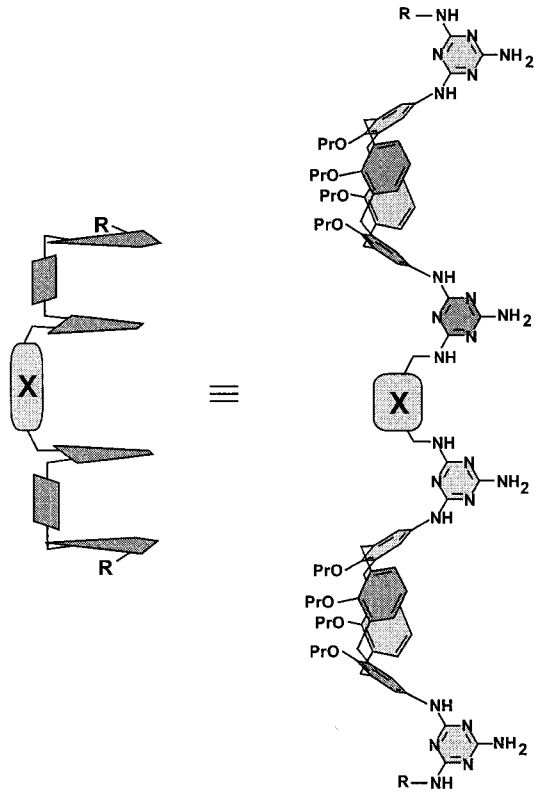

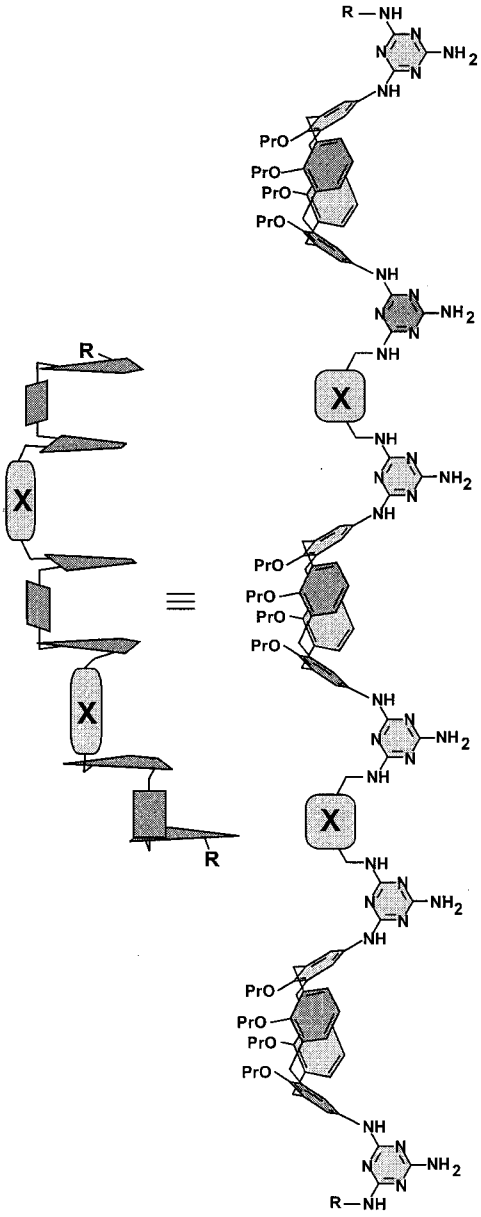

2a **R** = $(R)\text{-}CH(C_6H_5)CH_3$

X =

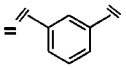

2b **R** = $(S)\text{-}CH(C_6H_5)CH_3$

X =

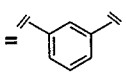

2c **R** = $(R)\text{-}CH(C_6H_5)CH_3$

X =

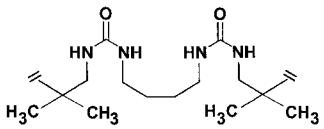

2d **R** =

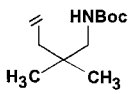

X =

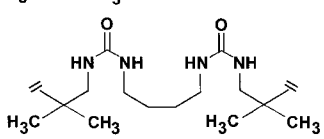

3a **R** = $(R)\text{-}CH(C_6H_5)CH_3$

X =

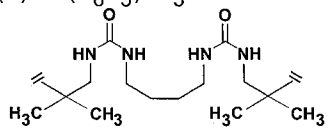

3b **R** =

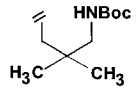

X =

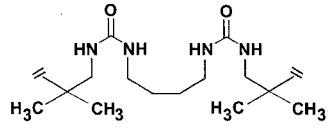

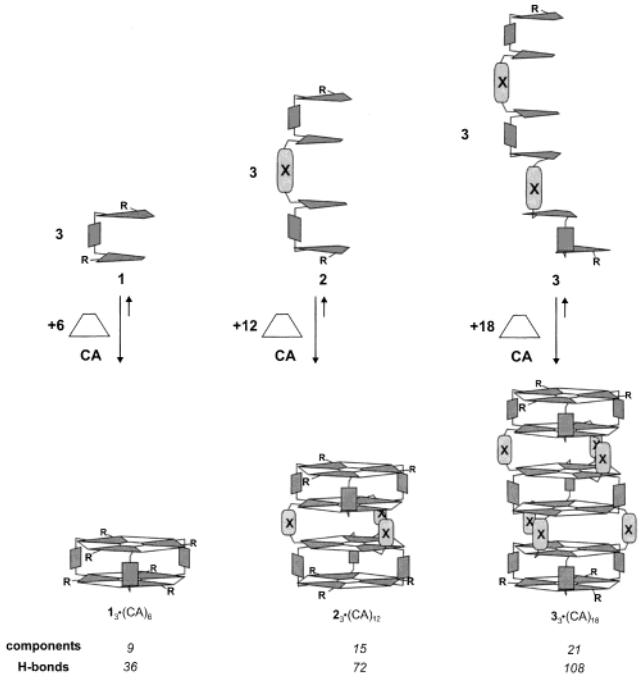

FIGURE 1. Schematic representations of double, tetra-, and hexarosette assemblies $\mathbf{1}_3$·$(CA)_6$, $\mathbf{2}_3$·$(CA)_{12}$, and $\mathbf{3}_3$·$(CA)_{18}$.

CHART 2

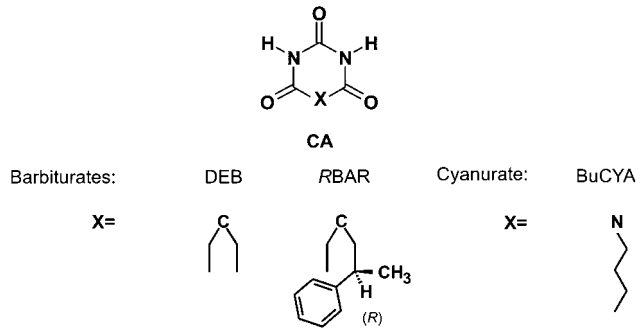

stabilities were measured either via racemization studies using enantiomerically pure assemblies or by means of chiral amplification studies by making use of the 'Sergeants and Soldiers' principle.[14,15]

Results and Discussion

Synthesis. For the induction of supramolecular chirality in tetra- and hexarosette assemblies by means of peripheral chiral substituents, several chiral analogues of tetramelamine **2** and hexamelamine **3** were synthesized. Two types of chiral tetramelamines **2** were examined, differing in the linker unit X connecting the two calix[4]arene dimelamines. The synthesis of tetramelamines **2a** and **2b**, having a rigid *m*-xylylene linker, started with the reaction of either **4a** or **4b**[16] with cyanuric chloride and gaseous NH_3 to give the corresponding intermediates $\mathbf{4a^I}$ and $\mathbf{4b^I}$. Subsequent reaction with an excess of *m*-xylylene diamine resulted in the formation of the corresponding dimelamines **5a** and **5b** in 68% yield (Scheme 1).[12] Subsequently, the enantiomeric tetramelamines **2a** and **2b** were obtained by coupling of intermediate $\mathbf{4a^I}$ with **5a** and of $\mathbf{4b^I}$ with **5b** in 82% and 62% yield, respectively.

The synthesis of chiral tetramelamine **2c** starts also from compound **4a**, but in this case 1,3-diamino-2,2-dimethylpropane was used to react with intermediate $\mathbf{4a^I}$ to give dimelamine calix[4]arene **6** (87%) (Scheme 2). Tetramelamine **2c** was obtained in 41% yield by reaction of **6** with 0.5 equiv of 1,4-diaminobutane bis(*p*-nitrophenyl dicarbamate). Achiral tetramelamine **2d** is synthesized (33%) from monoBoc-protected dimelamine **1e** and 1,4-butyl-bis(*p*-nitrophenyl) dicarbamate in CH_2Cl_2.

Hexamelamine **3a** was synthesized in 79% yield via coupling of diamino dimelamine **8** with 2 equiv of **7**, obtained by addition of excess of 1,4-diaminobutane bis(*p*-nitrophenyl dicarbamate) to **6** in 42% yield (Scheme 2). The synthesis of achiral hexamelamine **3b** is achieved by coupling of monoBoc dimelamine **1f** with **8**.

Tetra- and Hexarosette Assembly Formation. Characterization by ^{1}H NMR Spectroscopy and MALDI-TOF Mass Spectrometry. The formation of tetrarosette assembly $\mathbf{2a}_3$·$(DEB)_{12}$ was studied by means of a ^{1}H NMR titration experiment. Upon addition of increasing amounts of DEB (1−12 equiv) to a 3.0 mM solution of tetramelamine **2a** in CD_2Cl_2, the ^{1}H NMR spectrum changed instantaneously in a similar manner as previously observed for double rosette assemblies $\mathbf{1}_3$·$(DEB)_6$ (Figure 2a).[17,18] In general, the ^{1}H NMR spectra did not change in time, which indicates that the thermodynamic equilibrium is reached within seconds after mixing. Instead of the broad and featureless ^{1}H NMR spectrum of free **2a**, sharp signals start to appear when >2 equiv of DEB were added, signifying the formation of a well-defined assembly. Remarkably, at <2 equiv of DEB only one broad NH_{DEB} proton signal is observed around 14 ppm, which suggests that no tetrarosette is present at this stage. In fact, previously reported experiments with an achiral tetramelamine **2** showed comparable results, which seemed to be related to the negative cooperativity between the two double rosette layers in tetrarosette assemblies comprising a *m*-xylylene spacer.[12]

The 1:4 stoichiometry of assembly $\mathbf{2a}_3$·$(DEB)_{12}$ was confirmed by integration of the proton signals for NH_{DEB} (*a*,*b*) and ArNH (*c*,*d*) of **2a**. The presence of four signals for the H-bonded NH_{DEB} protons *a* and *b* at 13.92 (2 overlapping signals), 13.08, and 13.04 ppm is very characteristic for tetrarosette assemblies and clearly illustrates the fact that the inner and outer rosette layers in assembly $\mathbf{2a}_3$·$(DEB)_{12}$ are different. Analogously, two proton signals are observed for the ArNH proton *c* (8.32 and 8.08 ppm) and the benzylic NH proton *δ* (7.72 and 7.66 ppm) of **2a**. Two aromatic signals are observed (5.94 and 5.79 ppm) upfield from the normal position at for proton H*g* of calix[4]arene **2a**, which is in accordance with the pinched cone conformation that the calix[4]arenes

(14) Green, M. M.; Rediy, M. P.; Johnson, R. J.; Darling, G.; O'Leary, D. J.; Willson, G. *J. Am. Chem. Soc.* **1989**, *111*, 6452−6454.
(15) Green, M. M.; Peterson, N. C.; Sato, T.; Teramoto, A.; Cook, R.; Lifson, S. *Science* **1995**, *268*, 1860−1866.
(16) Prins, L. J.; Jolliffe, K. A.; Hulst, R.; Timmerman, P.; Reinhoudt, D. N. *J. Am. Chem. Soc.* **2000**, *122*, 3617−3627.
(17) Vreekamp, R. H. *Hydrogen-Bonded Assemblies of Calixarenes*; Thesis University of Twente: Enschede, The Netherlands, 1995; Chapter 6, ISBN 90-9008802-4.
(18) Vreekamp, R. H.; Van Duynhoven, J. P. M.; Hubert, M.; Verboom, W.; Reinhoudt, D. N. *Angew. Chem.* **1996**, *108*, 1306−1309; *Angew. Chem. Int. Ed. Engl.* **1996**, *35*, 1215−1218.

SCHEME 1. Synthesis of Tetramelamines 2a and 2b[a]

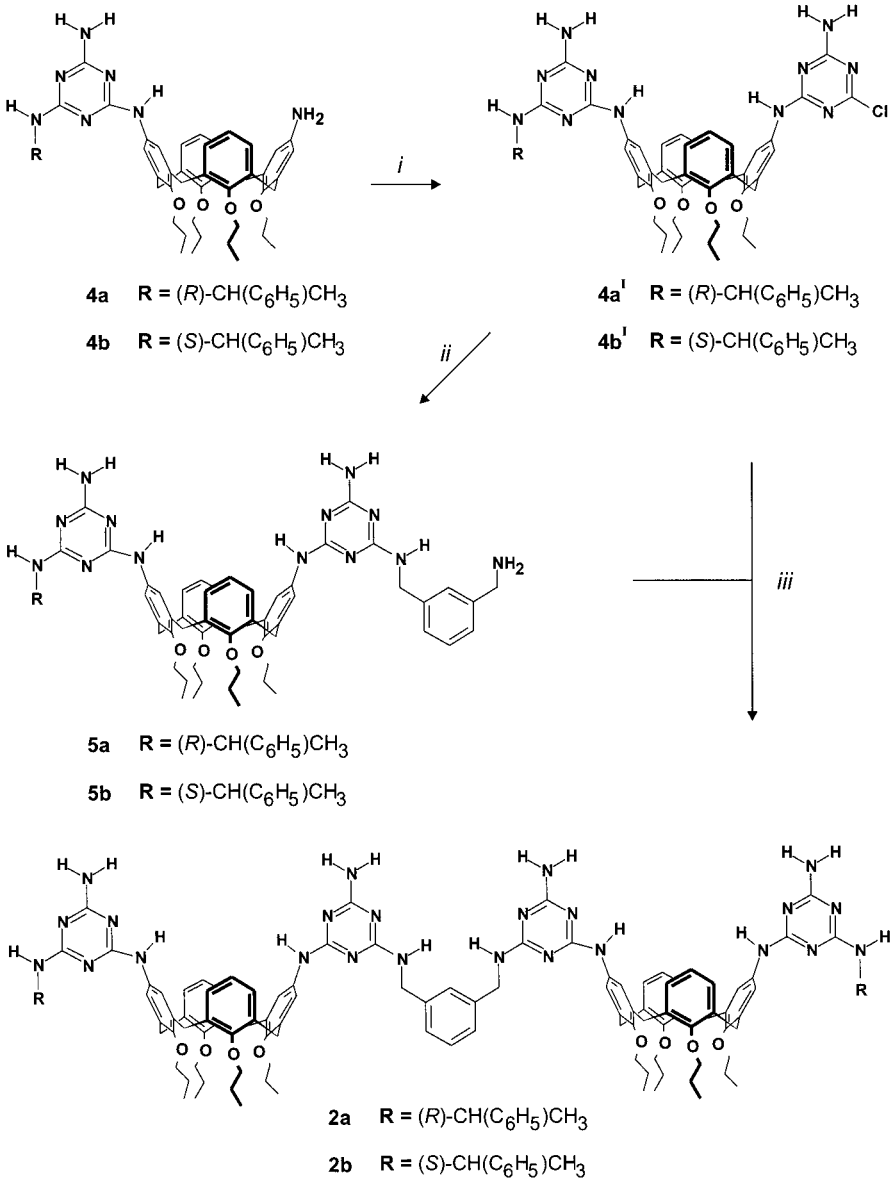

[a] (i) (1) Cyanuric chloride, 3 h, 0 °C, DIPEA, THF (2) NH_3 (g), 2H, 0 °C; (ii) *m*-xylylenediamine, 70 °C, 12 h; (iii) DIPEA, THF, 7 days, reflux

adopt, very similar to that observed for double rosette assemblies.[19] The other aromatic proton H*h* resonates at much lower field around 7.0 ppm, which is due to the formation of a weak H-bond with the nitrogen of the triazine that is not involved in H-bonding within the rosette. Interestingly, a strongly upfield shifted signal is present at 0.08 ppm, corresponding to half of the methyl groups of the DEB units (18 H) that are located in the inner rosette layers (2 and 3). Previously reported gas-phase minimization studies on a related assembly have indicated that these protons point right into the face of one of aromatic rings of the calix[4]arene fragments.[12]

Assemblies $\mathbf{2a}_3$·$(DEB)_{12}$ and $\mathbf{2b}_3$·$(DEB)_{12}$ have identical ^1H NMR spectra since these assemblies are enantiomers. The ^1H NMR spectrum of assembly $\mathbf{2c}_3$·$(DEB)_{12}$ shows all the characteristic tetrarosette signals as described for the structurally related assembly $\mathbf{2d}_3$·$(DEB)_{12}$.

Mixing of hexamelamine **3a** and DEB in a 1:6 ratio results in the quantitative formation of hexarosette assembly $\mathbf{3a}_3$·$(DEB)_{18}$, similarly to assembly $\mathbf{3b}_3$·$(DEB)_{18}$. The highly symmetric nature of this assembly (vide infra) makes that the ^1H NMR spectrum is remarkably easy to interpret, especially when considering the fact that the assembly comprises 21 components that are held together by 108 H-bonds (Figure 3). The 1:6 stoichiometry of assembly $\mathbf{3a}_3$·$(DEB)_{18}$ was confirmed by integration of the NH_{DEB} and the calix[4]arene CH_2 bridge proton signals. As a result of the fact that assembly $\mathbf{3a}_3$·$(DEB)_{18}$ comprises three chemically different rosette layers, a total of six different proton signals is observed for the NH_{DEB} protons at 14.10, 13.76, 13.72, 13.04 (double intensity), and 12.97 ppm. Other characteristic signals include the

(19) Arduini, A.; Fanni, S.; Manfredi, G.; Pochini, A.; Ungaro, R.; Sicuri, A.-R.; Ugozzoli, F. *J. Org. Chem.* **1995**, *60*, 1448.

SCHEME 2. Synthesis of Chiral Tetramelamine 2c and Chiral Hexamelamine 3a[a]

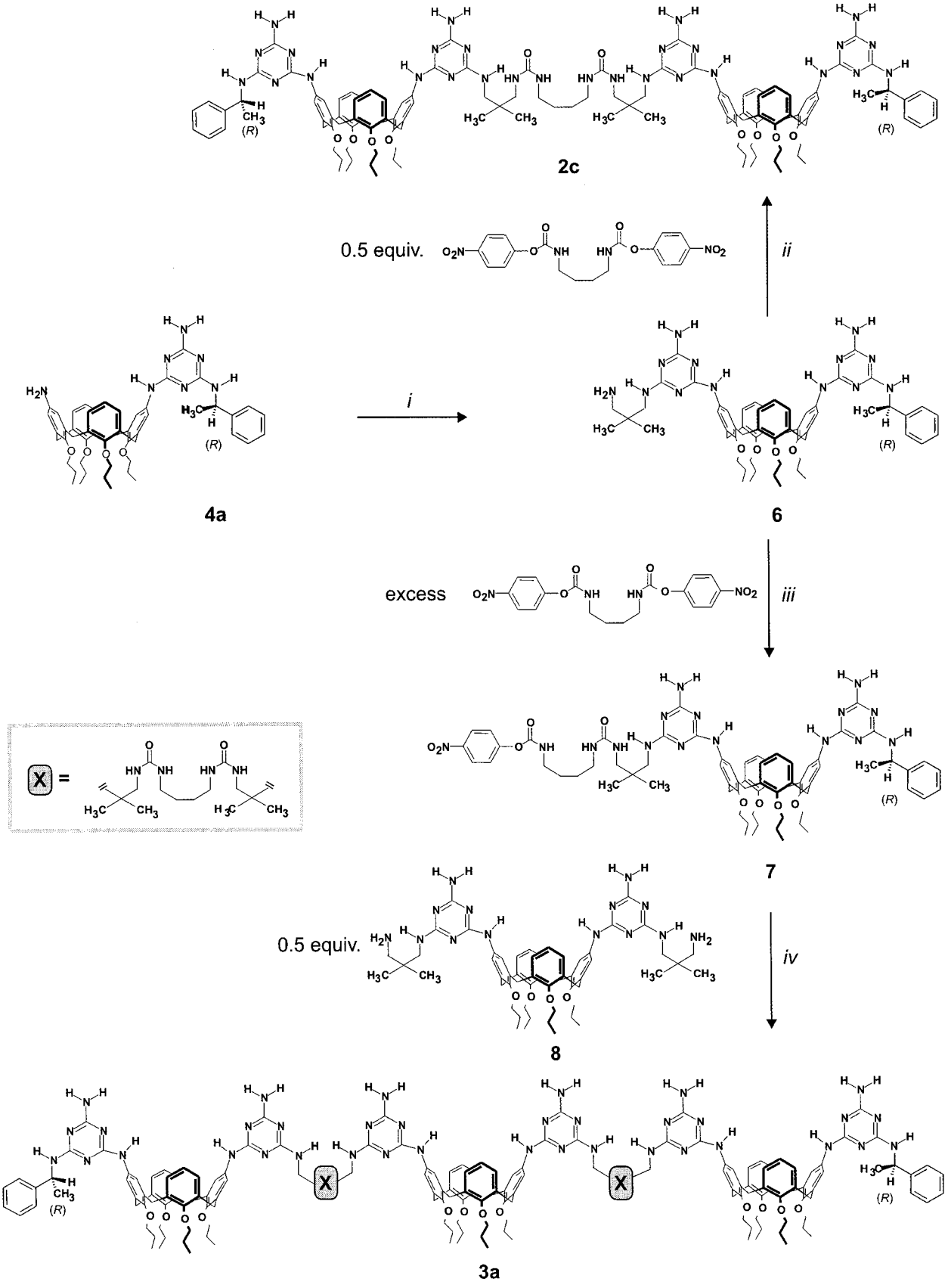

[a] (i) (1) Cyanuric chloride, 3 h, 0 °C, DIPEA, THF, (2) NH_3 (g), 2 H, 0 °C, (3) 1,3-diamino-2,2-dimethylpropane, 70 °C, 12 h; (ii) 1,4-diaminobutane bis(*p*-nitrophenyl) dicarbamate (0.5 equiv),[13] DIPEA, acetone, CH_2Cl_2, reflux, 12 h; (iii) 1,4-diaminobutane bis(*p*-nitrophenyl dicarbamate) (excess), DIPEA, acetone, CH_2Cl_2, reflux, 12 h; (iv) DIPEA, CH_2Cl_2, reflux, 12 h.

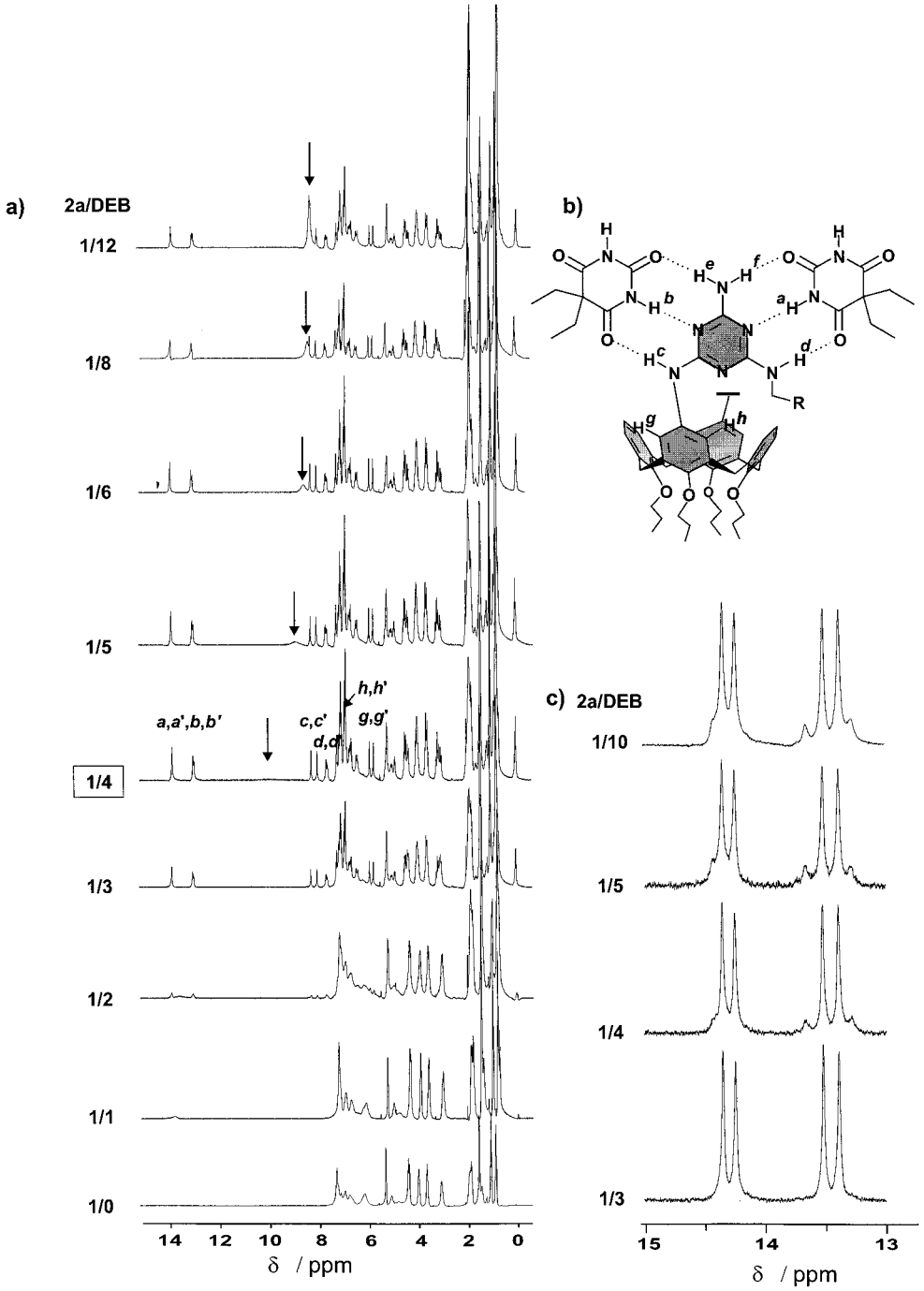

FIGURE 2. (a) ^{1}H NMR titration of tetramelamine **2a** with DEB in CD_2Cl_2 ([**2a**] = 3.0 mM). Arrows indicate NH proton signal for 'free' DEB. (b) Protons of assembly **2a**$_3$·(DEB)$_{12}$ that give characteristic signals in the ^{1}H NMR spectrum. For each proton, two different signals are observed, the result of the fact that the four rosette motifs in **2a**$_3$·(DEB)$_{12}$ are pairwise different. (c) ^{1}H NMR titration of tetramelamine **2a** with DEB in toluene-d_8 ([**2a**] = 3.0 mM).

three signals at 8.61, 8.51, and 8.02 ppm for the ArNH protons and the combined signals at 7.70, and 7.63 (double intensity) ppm for the benzylic NH protons of **3a**.

Additional evidence for the formation of tetrarosettes **2a**$_3$·(DEB)$_{12}$, **2b**$_3$·(DEB)$_{12}$, and **2c**$_3$·(DEB)$_{12}$ and hexarosette **3a**$_3$·(DEB)$_{18}$ was obtained from MALDI-TOF mass spectrometry measurements after Ag^+-labeling.[12,20] The results of these measurements are given in Table 1. In all cases were observed intense signals for the monovalent Ag^+-complexes of the assemblies, although it should be noted that in most cases low-intensity signals were also present at lower *m*/*z* ratios. The origin of these signals remains unclear, as the signals could not be attributed to partly formed assemblies. Assemblies **2d**$_3$·(DEB)$_{12}$ and **3b**$_3$·(DEB)$_{18}$ lack binding sites for Ag^+ (i.e., π-arene, π-alkene donor functionalities and/or cyano and crown ether functionalities) and therefore could not be detected by MALDI-TOF MS.

(20) Timmerman, P.; Jolliffe, K. A.; Crego-Calama, M.; Weidmann, J.-L.; Prins, L. J.; Cardullo, F.; Snellink-Ruel, B. H. M.; Fokkens, R.; Nibbering, N. M. M.; Shinkai, S.; Reinhoudt, D. N. *Chem. Eur. J.* **2000**, *6*, 4104−4115.

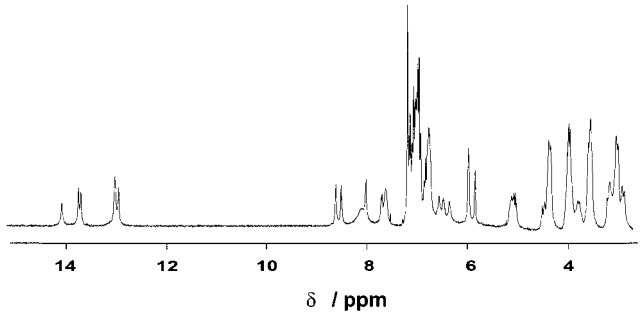

FIGURE 3. ^{1}H NMR spectrum of hexarosette assembly $\mathbf{3a}_3$·$(DEB)_{18}$ in $CDCl_3$ (1.0 mM) at room temperature.

TABLE 1. Results of MALDI-TOF MS Measurements

assembly	molecular formula	calcd mass (Da)	obsd mass (Da)
$\mathbf{2a}_3$·$(DEB)_{12}$·Ag^+	$C_{444}H_{546}O_{60}N_{96}Ag$	8295.8	8296.3[a]
$\mathbf{2b}_3$·$(DEB)_{12}$·Ag^+	$C_{444}H_{546}O_{60}N_{96}Ag$	8295.8	8294.7[a]
$\mathbf{2c}_3$·$(DEB)_{12}$·Ag^+	$C_{468}H_{618}O_{66}N_{108}Ag$	8920.7	8921.2
$\mathbf{3a}_3$·$(DEB)_{18}$·Ag^+	$C_{702}H_{948}O_{102}N_{168}Ag$	13480.3	13479.6[b]

[a] Low intensity signals in the 4000−6000 *m*/*z* region were observed. [b] An additional signal at *m*/*z* 6626.6 was observed.

Additional Complexation of DEB by Tetrarosette Assembly $\mathbf{2a}_3$·$(DEB)_{12}$. The signal of the NH protons of 'nonassembled' DEB ($NH_{DEB,non}$) shows completely different behavior in the ^{1}H NMR titration of tetramelamine **2a** with DEB as compared to previously reported double rosette titration experiments (Figure 2).[17,18] This signal usually appears when more than stoichiometric amounts of DEB are added to melamine (>2 equiv for dimelamine **1**, >4 equiv for tetramelamine **2**). In the double rosette studies the $NH_{DEB,non}$ proton signal was observed at 8.4 ppm and found to be independent of the amount of excess of DEB present. However, in case of tetramelamine **2a** the $NH_{DEB,non}$ signal was observed at 9.8 ppm (1:4 ratio of **2a** and DEB), while the signal ultimately was shifted to 8.36 ppm in the presence of 12 equiv of DEB. This leads to the conclusion that exchange between assembled and 'nonassembled' DEB is slow on the chemical shift time scale, but that the 'nonassembled' DEB is also involved in the formation of an additional complex with the tetrarosette, the formation of which is fast on the chemical shift time scale. Structural evidence for the complex is still missing, but we believe that the complex formation involves the binding of a DEB unit to one of the outer rosette layers (1 and 4). This type of complex formation could be somehow related to the observed 'catalytic' behavior of free barbiturates in the racemization of double rosette assemblies $\mathbf{1}_3$·$(DEB)_6$.[10] The exact mode of binding is still unknown, but it seems likely that the melamine units that are involved in rosette formation may still possess sufficient H-bonding capacity to bind to free DEB. However, it is quite remarkable that this type of binding was never observed for double rosettes. It could be that the *m*-xylylene spacers in **2a** are somehow responsible for the observed phenomenon as we know that they induce negative cooperativity between the two rosette layers (vide supra).[12] Doing so, they could potentially reduce the effectiveness for H-bonding between melamines and DEB within the rosettes and thus stimulate the binding of the melamine units to 'nonassembled' DEB.

TABLE 2. Number of Expected NH_{DEB} Proton Signals for All Possible Isomers of Tetrarosette Assemblies $\mathbf{2}_3$·$(CA)_{12}$

	number of expected NH_{DEB} signals[a]					
substituent R	SSS	SES	SSE	SEE	ESE	EEE
achiral	4	4	8	8	8	4
chiral	4[b]	8	8[b]	8[b]	8[b]	8

[a] The three-letter codes refer to the isomers depicted in Figure 8.4 (S: staggered; E: eclipsed). [b] For each diastereomer.

To obtain additional information about the nature of this complex a titration experiment was performed in toluene-d_8, in which the kinetics for assembly are much slower than for chloroform. A mixture of tetramelamine **2a** and DEB in a 1:3 ratio exclusively shows signals for the NH_{DEB} protons *a* and *b* at 14.40, 14.29, 13.56, and 13.43 ppm, which indicates that all DEB is assembled in tetrarosette $\mathbf{2a}_3$·$(DEB)_{12}$ (Figure 2c). However, upon increasing the amount of DEB, small additional signals appear, indicating the formation of a new tetrarosette assembly. The fact that two sets of tetrarosette signals are observed, shows that these assemblies are in slow exchange on the chemical shift time scale. Since the intensities of these new signals vary with the concentration of DEB, it seems likely to conclude that tetrarosette $\mathbf{2a}_3$·$(DEB)_{12}$ and free DEB form a complex, i.e. $\mathbf{2a}_3$·$(DEB)_{12}$·DEB. Fortunately, the formation of this complex does not complicate our studies of the chiral induction in tetrarosette assemblies to any extent, since at a 1:4 ratio of **2a** and DEB the signals corresponding to complex $\mathbf{2a}_3$·$(DEB)_{12}$·DEB only account for <5% of the total assembly concentration.

Induction of Supramolecular Chirality in Tetra- and Hexarosette Assemblies. Principally, tetrarosette and hexarosette assemblies can adopt a large variety of different isomeric structures as the melamines in each rosette layer can adopt either a staggered (S) or an eclipsed (E) conformation.[21] As an illustration of this potential problem all possible tetrarosette isomers are schematically depicted in Figure 4. Just like for double rosette assemblies, the number of NH_{DEB} proton signals in the ^{1}H NMR spectrum provides important information regarding the symmetry of the assemblies.[22] In Table 2 the number of expected NH_{DEB} signals for all tetrarosette isomers are listed, both for chiral and achiral melamines. From these data it immediately becomes clear that the four different NH_{DEB} proton signals observed for assemblies $\mathbf{2a}_3$·$(DEB)_{12}$, $\mathbf{2b}_3$·$(DEB)_{12}$, and $\mathbf{2c}_3$·$(DEB)_{12}$ (vide supra) indicate the exclusive formation of the SSS-isomer, either with *M*- or *P*-chirality. Just like for double rosette assemblies[23] the presence of six chiral centers induce one single handedness in tetrarosette assemblies in a quantitative sense (>98%), as proton signals for the diastereomeric assembly with opposite chirality were not observed. The extent of chiral induction appears to be independent of the linker unit X between rosette layers 2 and 3. Similarly, the supramolecular chirality of hexarosette assembly $\mathbf{3a}_3$·$(DEB)_{18}$, having a molecular

(21) For an extensive discussion of isomerism in double rosette assemblies $\mathbf{1}_3$·$(CA)_6$, see ref 16.

(22) Chin, D. N.; Simanek, E. E.; Li, X.; Wazeer, M. I. M.; Whitesides, G. M. *J. Org. Chem.* **1997**, *62*, 1891−1895.

(23) Prins, L. J.; Huskens, J.; De Jong, F.; Timmerman, P.; Reinhoudt, D. N. *Nature* **1999**, *398*, 498−502.

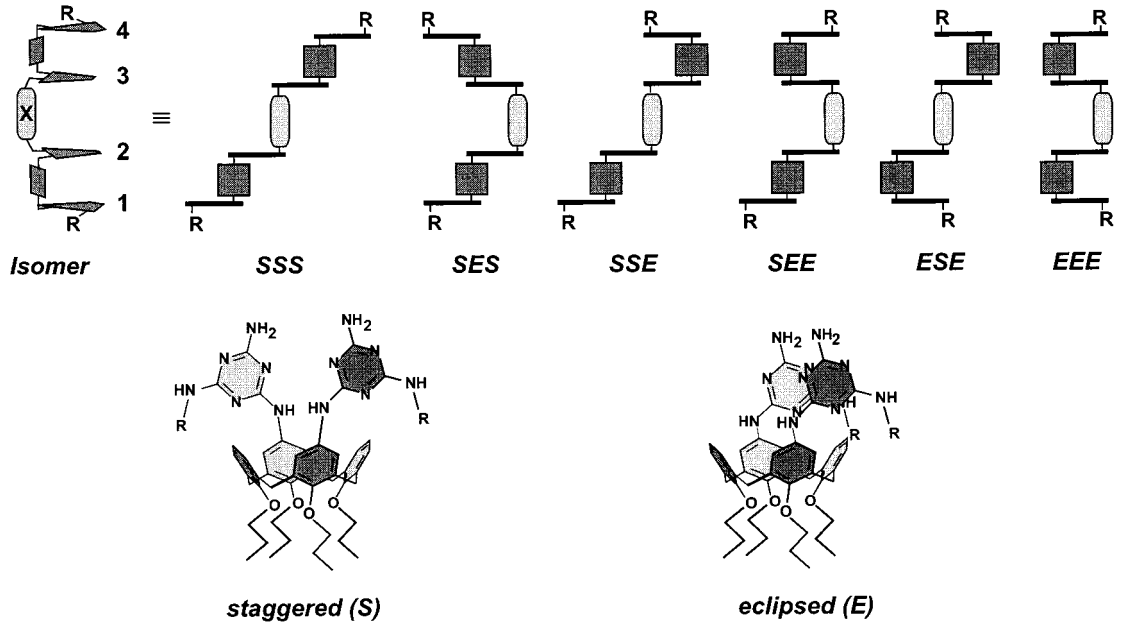

FIGURE 4. Schematic representations of all possible isomers of a tetrarosette assembly. Only assemblies having a C_3-symmetry axis are considered, which means that all three tetramelamine strands have the same orientation. The three-letter code (*S* for staggered; *E* for eclipsed) represents the relative orientation of the melamine fragments for each rosette layer. The *SSS*, *SSE*, *SEE*, and *ESE* isomers are chiral and, therefore, are present as a racemic mixture of the *M*- and *P*-enantiomer (not shown).

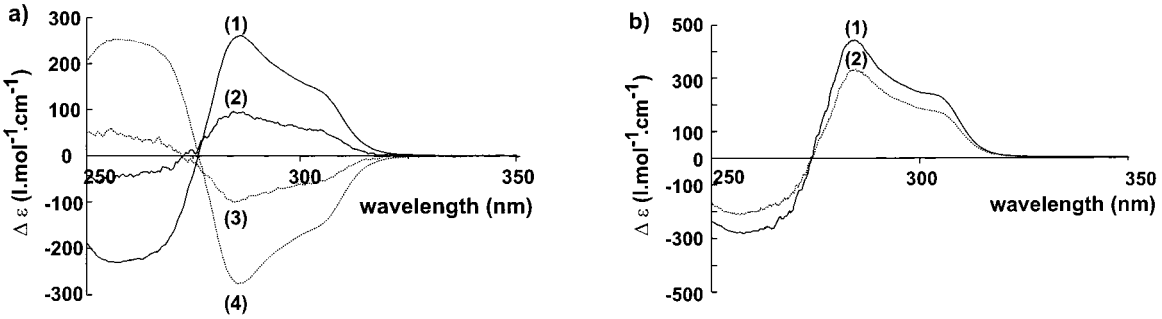

FIGURE 5. (a) CD spectra of tetrarosette assemblies *M*-**2a**$_3$·(DEB)$_{12}$ (1) and *P*-**2b**$_3$·(DEB)$_{12}$ (4) and double rosette assemblies *M*-**1a**$_3$·(DEB)$_6$ (2) and *P*-**1b**$_3$·(DEB)$_6$ (3). All spectra were recorded in CH_2Cl_2 (1.0 mM) at room temperature. (b) CD spectra of hexarosette assembly *M*-**3a**$_3$·(DEB)$_{18}$ (1) and tetrarosette assembly *M*-**2c**$_3$·(DEB)$_{12}$ (2). Both spectra were recorded in $CHCl_3$ (1.0 mM) at room temperature.

weight of 13480 Da, is quantitatively induced by only six chiral centers.

The chiroptical activity of the assemblies was studied by CD spectroscopy. Tetrarosette assemblies **2a**$_3$·(DEB)$_{12}$ and **2b**$_3$·(DEB)$_{12}$ display a mirror image CD curve, which clearly reflects their enantiomeric relationship (Figure 5a). Comparison of the CD spectra of tetrarosette assembly **2a**$_3$·(DEB)$_{12}$ and double rosette assembly **1a**$_3$·(DEB)$_6$ shows that the (*R*)-1-phenylethyl substituents induce *M*-chirality in both assemblies, as the spectra have equal signs. Moreover, the CD curves are very similar in shape (*x*-axis cutoff at 276 nm and maxima at 257, 286, and 306 nm), which indicates the high structural similarity between the assemblies. The CD intensity of tetrarosette **2a**$_3$·(DEB)$_{12}$ at wavelengths <276 nm is relatively high, which might be due to the presence of the *m*-xylylene linker. The CD intensity of **2a**$_3$·(DEB)$_{12}$ ($\Delta\epsilon_{286}$ = 259.7 L mol^{-1} cm^{-1}) is significantly higher than that of **1a**$_3$·(DEB)$_6$ ($\Delta\epsilon_{286}$ = 100 L mol^{-1} cm^{-1}) despite the fact that both assemblies contain only six chiral substituents. This provides additional proof for earlier reported conclusions that the high CD activity observed for rosette assemblies is mainly the result of chiral exciton coupling of chromophores within the core of the assembly.[23,24] The difference in CD intensity of tetrarosette **2a**$_3$·(DEB)$_{12}$ and **2c**$_3$·(DEB)$_{12}$ ($\Delta\epsilon_{max}$ = 327.9 L mol^{-1} cm^{-1}) is attributed to the different linker units X (*m*-xylylene vs urea's), which have different chromophoric units that intrinsically cause a different CD intensity. Also the different length and rigidity is likely to affect the orientation between the rosette layers (2 and 3).

As expected, the CD spectra of the closely related tetrarosette **2c**$_3$·(DEB)$_{12}$ and hexarosette **3a**$_3$·(DEB)$_{18}$ exhibit bisignate curves characteristic for rosette assemblies (Figure 5b). The positive sign reveals that both assemblies have induced *M*-chirality. As a result of the presence of six rosette layers, hexarosette **3a**$_3$·(DEB)$_{18}$ exhibits a much higher CD intensity ($\Delta\epsilon_{284}$ = 439.7 L

(24) Prins, L. J.; Thalacker, C.; Würthner, F.; Timmerman, P.; Reinhoudt, D. N. *Proc. Natl. Acad. Sci. U.S.A.* **2001**, *98*, 10042−10045.

mol^{-1} cm^{-1}) than tetrarosette assembly **2a**$_3$·(DEB)$_{12}$ ($\Delta\epsilon_{max}$ = 259.7 L mol^{-1} cm^{-1}).

Chiral Amplification Experiments with Tetrarosette Assemblies. Both ^{1}H NMR and CD spectroscopic studies of tetra- and hexarosette assemblies show that the assemblies behave very much like double rosette assemblies, at least under equilibrium conditions. However, the kinetic stability of tetrarosette assemblies is significantly higher than for double rosettes as a result of the larger number of H-bonds involved in assembly formation. The kinetic stability of tetrarosette assemblies was studied by performing 'Sergeants and Soldiers' experiments. Previous studies with mixtures of double rosette assemblies *M*-**1a**$_3$·(BuCYA)$_6$ and achiral **1c**$_3$·(BuCYA)$_6$[25] revealed a nonlinear relationship between the CD intensity of the mixture and the ratio of *M*-**1a**$_3$·(BuCYA)$_6$:**1c**$_3$·(BuCYA)$_6$.[23,25] This nonlinear behavior is the direct result of the presence of heteromeric assemblies **1a**$_2$**1c**$_1$·(BuCYA)$_6$ and **1a**$_1$**1c**$_2$·(BuCYA)$_6$, formed via exchange of the dimelamines **1a** and **1c** from the homomeric assemblies. In the heteromeric assemblies the achiral dimelamines **1c** 'follow' the chirality induced by the chiral dimelamines **1a**.

The studies were performed both in chloroform and benzene. It was found that exchange of the dimelamines **1a** and **1c** is very slow in benzene, which allows the increase in CD intensity to be followed in time. The kinetic model A[30] was used to describe this process, assuming that dissociation of the first dimelamine (with rate constant $k_{dis,m}$) from an intact assembly is the rate determining step. The kinetic model A describes all relevant dissociations and associations that occur in the mixture of chiral and achiral dimelamines. The mixture is treated as an equilibrating system containing eight different assemblies **1**$_3$·(BuCYA)$_6$, three intermediates assemblies (lacking one dimelamine component) **1**$_2$·(BuCYA)$_6$, and the free components **1a** and **1c**.

Fitting of the experimental data to model A gave a value for $k_{dis,m}$ = (4.6 ± 0.9) × 10^{-4} s^{-1} in benzene at 70 °C. The excellent fits observed provide evidence for the fact that the minimal model A gives a proper description of the kinetic processes that occur upon mixing assemblies *M*-**1a**$_3$·(BuCYA)$_6$ and **1c**$_3$·(BuCYA)$_6$.

To be able to determine a $k_{dis,m}$ value for tetrarosette assemblies, we planned to run a similar set of 'Sergeants and Soldiers' experiments with the tetrarosette assemblies *M*-**2c**$_3$·(BuCYA)$_{12}$ and achiral **2d**$_3$·(BuCYA)$_{12}$. Unfortunately, it turned out to be practically impossible to achieve the clean formation of cyanurate-based assemblies **2**$_3$·(BuCYA)$_{12}$ by the direct mixing of tetramelamines **2** and BuCYA.[13] For this reason, the 'Sergeants and Soldiers' experiments were performed with assemblies *M*-**2c**$_3$·(DEB)$_{12}$ and **2d**$_3$·(DEB)$_{12}$. Solutions of *M*-**2c**$_3$·(DEB)$_{12}$ and achiral **2d**$_3$·(DEB)$_{12}$ in chloroform (1.0 mM) were mixed in a 40:60 ratio, and the CD intensity was measured as a function of time at different temperatures. The relative CD intensities were calculated assuming equal CD intensities for all assemblies present (Figure 6a).[26] The resulting curves are very similar to those obtained for double rosette assemblies, which indicates that chiral amplification in tetrarosettes occurs in a similar manner. The resulting plots were fitted to model A using linear regression analysis, which gave the $k_{dis,m}$ values as presented in Table 3. From a plot of ln $k_{dis,m}$ versus 1/*T* an activation energy of 98.7 ± 16.6 kJ mol^{-1} for the dissociation of tetramelamine **2** from tetrarosette assembly **2c**$_3$·(DEB)$_{12}$ was calculated using Arrhenius's equation ($k_{dis.m} = Ae^{-E_{act}/RT}$) (Figure 6b).

TABLE 3. Values for $k_{dis,m}$ in Chloroform and Benzene as Obtained from Fitting the Results to Model A for Tetramelamines 2c and 2d in Assemblies 2c$_n$2d$_{3-n}$·(BuCYA)$_{12}$ (n = 0−3)

T (°C)	$k_{dis,m}$ (× 10^{-5} s^{-1}) chloroform	$k_{dis,m}$ (× 10^{-5} s^{-1}) benzene
25	2.8 ± 0.6	-
35	4.9 ± 0.4	-
45	38.1 ± 7.0	-
50	-	1.3 ± 0.1
55	78.6 ± 6.8	3.7 ± 0.1
60	-	6.8 ± 0.1
65	-	19.7 ± 0.1
70	-	63.4 ± 0.8

To study the effect of solvent on the kinetic parameters for assembly, the same set of experiments was also performed in benzene, a solvent that is known to enhance the stability of H-bonds. The measurements were performed at temperatures ranging from 50 to 70 °C, because at lower temperatures the increase in CD intensity was too slow (Figure 6c). The results were fitted to model A, giving the $k_{dis,m}$ values as presented in Table 3. From these data, an activation energy of 172.8 ± 11.3 kJ mol^{-1} was determined (Figure 6d). This value clearly shows the enormous enthalpy price that must be paid in order to dissociate a tetramelamine from a tetrarosette assembly in benzene, a process that involves the disruption of 24 H-bonds.

Racemization Studies of Double, Tetra- and Hexarosette Assemblies. Previously, we measured the activation energy for the racemization of enantiomerically pure assembly *P*-**1d**$_3$·(BuCYA)$_6$ (105.9 ± 6.4 kJ mol^{-1}) by means of variable temperature studies.[10] We now used similar racemization studies for enantiomerically enriched tetra- and hexarosette in order to be able to determine how the kinetic stabilities of double, tetra- and hexarosettes are related.

Enantiomerically enriched tetrarosette *P*-**2d**$_3$·(BuCYA)$_{12}$ and hexarosette *P*-**3b**$_3$·(BuCYA)$_{18}$ assemblies were prepared in the same way as described previously for double rosette assembly *P*-**1d**$_3$·(BuCYA)$_6$.[10,11] The supramolecular chirality of the assemblies is induced by using chiral barbiturate *R*BAR, which are subsequently replaced by achiral BuCYA. Assembly of tetramelamine **2d** with 4

(25) Prins, L. J.; Hulst, R.; Timmerman, P.; Reinhoudt, D. N. *Chem. Eur. J.* **2002**, *8*, 2288−2301.

(26) The presence of different chromophores in tetramelamines **2c** and **2d** might cause a small difference in CD intensity for corresponding assemblies. However, for the determination of k_{dism}, the relative CD intensity is not so important, since it only affects the f_m value in model A and not k_{dism}.

(27) Integration of the proton signals in the 13−15 ppm corresponds to six protons, despite the fact that only four signals are observed.

(28) The effect of the presence of *R*BAR on the racemization rate is reflected by the calculated half-lifes to racemization of double rosette *P*-**1d**$_3$·(BuCYA)$_6$ of 46 s and 9.6 h for the catalyzed and uncatalyzed pathway, respectively (based on k_{cat} = (7.5 ± 0.8) × 10^{-3} L mol^{-1} s^{-1} and k_{uncat} = (1.0 ± 0.6) × 10^{-5} s^{-1}).

(29) Timmerman, P.; Vreekamp, R. H.; Hulst, R.; Verboom, W.; Reinhoudt, D. N.; Rissanen, K.; Udachin, K. A.; Ripmeester, J. *Chem. Eur. J.* **1997**, *3*, 1823−1832.

(30) Prins, L. J.; Timmerman, P.; Reinhoudt, D. N. *J. Am. Chem. Soc.* **2001**, *123*, 10153−10163.

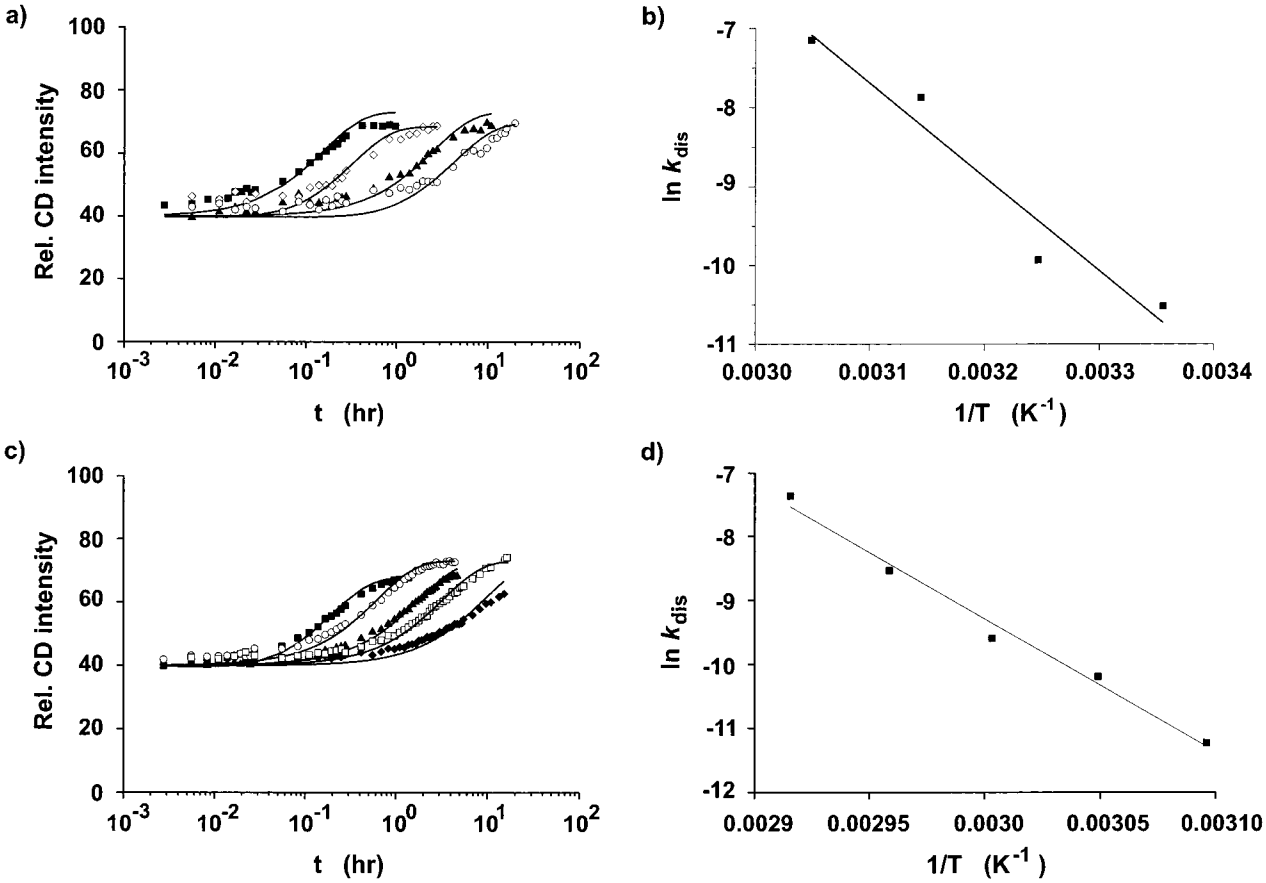

FIGURE 6. (a) Increase in CD intensity in time upon mixing assemblies *M*-**2c**$_3$·(DEB)$_{12}$ and **2d**$_3$·(DEB)$_{12}$ in a 40:60 ratio in chloroform (1.0 mM) at 25 (○), 35 (▲), 45 (◊), and 55 (■) °C. The lines represent calculated values obtained after fitting the experimental data to model A.[30] (b) Plot of ln $k_{dis,m}$ vs 1/*T* for the values obtained in chloroform. (c) Increase in CD intensity for the same mixture in benzene (1.0 mM) at 50 (♦), 55 (□), 60 (▲), 65 (○), and 70 (■) °C. (d) Plot of ln $k_{dis,m}$ vs 1/*T* for the values obtained in benzene.

equiv of *R*BAR results in the quantitative formation of assembly **2d**$_3$·(*R*BAR)$_{12}$, as evidenced by integration of the proton signals for NH_{RBAR} and the calix[4]arene CH_2 bridge protons of **2d** (Figure 7a). Additional evidence for the formation of assembly **2d**$_3$·(*R*BAR)$_{12}$ was obtained by MALDI-TOF mass spectrometry. After the assembly was labeled with Ag^+, an intense signal was observed at *m*/*z* 10489, which corresponds to the presence of the monovalent Ag^+-complex of assembly **2d**$_3$·(*R*BAR)$_{12}$ (calcd for $C_{564}H_{756}N_{114}O_{78}Ag$ = 10488.9).

The large number of signals observed for the NH_{RBAR} protons are presumably due to the different possible orientations of the *R*BAR components in the assembly. Although this prevents the exact determination of the de for assembly **2d**$_3$·(*R*BAR)$_{12}$, the rate constant for racemization can still be determined as the rate constant is independent of the initial concentrations of the enantiomers. More importantly, the assembly displays a CD activity ($\Delta\epsilon_{270}$ = 357.4 L mol^{-1} cm^{-1}) similar to that of tetrarosette assembly *M*-**2c**$_3$·(DEB)$_{12}$, which indicates a similar degree of chiral induction, i.e., close to quantitative (Figure 8). The negative sign of the CD curve shows that *R*BAR induces *P*-helicity in assembly **2d**$_3$·(*R*BAR)$_{12}$

Enantiomerically enriched tetrarosette assembly *P*-**2d**$_3$·(BuCYA)$_{12}$ was prepared by adding 1.2 equiv of BuCYA (relative to *R*BAR) to a 1.0 mM solution of *P*-**2d**$_3$·(*R*BAR)$_{12}$ in chloroform-*d*. The ^{1}H NMR spectrum after

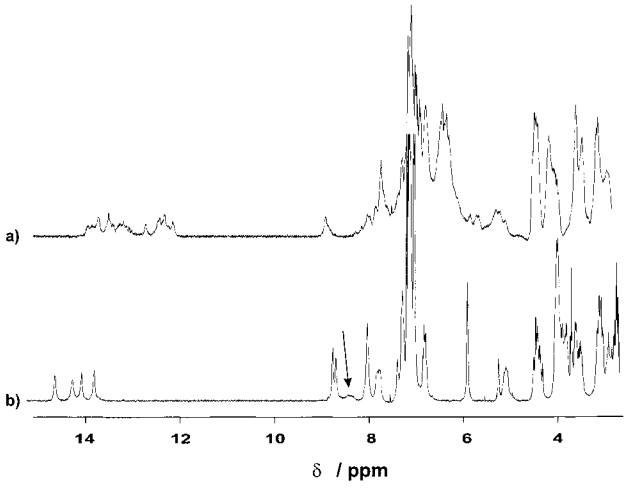

FIGURE 7. (a) ^{1}H NMR spectrum of assembly *P*-**2d**$_3$·(*R*BAR)$_{12}$ in $CDCl_3$ (1.0 mM) at room temperature. (b) The same mixture after addition of 1.2 equiv of BuCYA (relative to *R*BAR). The broad signal indicated with an arrow originates from the NH protons of expelled *R*BAR.

exchange only shows the characteristic tetrarosette signals, indicating that assembly *P*-**2d**$_3$·(BuCYA)$_{12}$ is formed as a well-defined assembly (Figure 7b), in sharp contrast to the very complex ^{1}H NMR spectrum obtained

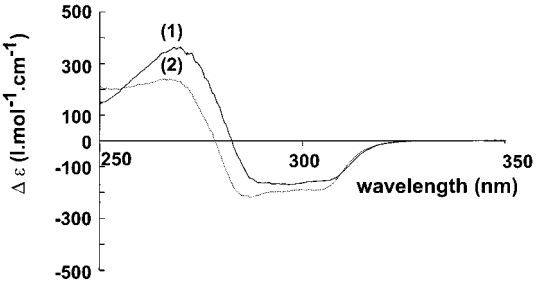

FIGURE 8. CD spectra of assemblies *P*-**2d**$_3$·(*R*BAR)$_{12}$ (1) and *P*-**2d**$_3$·(BuCYA)$_{12}$ (2), prepared via addition of 1.2 equiv of BuCYA to assembly *P*-**2d**$_3$·(*R*BAR)$_{12}$. Both spectra were recorded in chloroform (1.0 mM) at room temperature.

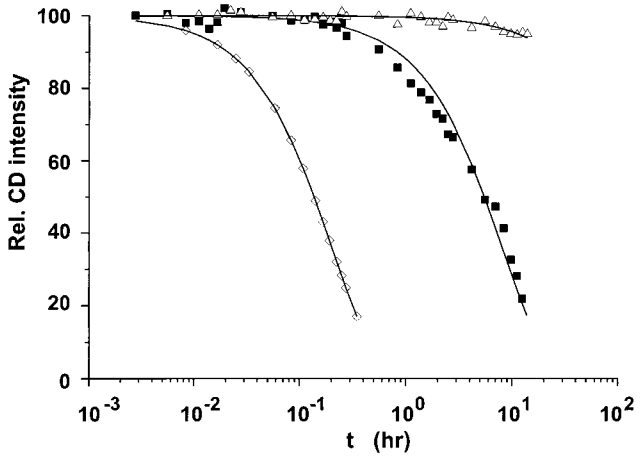

FIGURE 9. Racemization of double rosette *P*-**1d**$_3$·(BuCYA)$_6$ (◊), tetrarosette *P*-**2d**$_3$·(BuCYA)$_{12}$ (■), and hexarosette *P*-**3b**$_3$·(BuCYA)$_{18}$ (△) in chloroform 1.0 mM at 50 °C. The lines represent calculated best fits to the racemization model.[10]

upon directly mixing tetramelamine **2d** and BuCYA.[13] Apparently, the clean synthesis of assembly *P*-**2d**$_3$·(BuCYA)$_{12}$ is only possible via an intermediate assembly comprised of barbiturates.

Assembly **2d**$_3$·(BuCYA)$_{12}$ still has a very high CD activity, which means that the *P*-chirality induced by *R*BAR in assembly *P*-**2d**$_3$·(*R*BAR)$_{12}$ is 'memorized' after exchange (Figure 8). Subsequently, the racemization rate of assembly *P*-**2d**$_3$·(BuCYA)$_{12}$ was measured by monitoring the decrease of the CD intensity in time in chloroform at 50 °C (Figure 9). The resulting curve was fitted to a racemization model, giving a racemization rate constant $k_{rac} = (1.8 \pm 0.1) \times 10^{-5}$ s^{-1}.[10] This corresponds to a racemization half-life of 5.5 h. For comparison, the racemization rate of double rosette *P*-**1d**$_3$·(BuCYA)$_6$ was measured under identical conditions, giving a $k_{rac} = (70.2 \pm 0.1) \times 10^{-5}$ s^{-1} with a corresponding half-life of 8.4 min. The racemization half-life of tetrarosettes is 40 times higher compared to double rosettes, as a direct result of the increased number of H-bonds that needs to be disrupted in order for racemization to occur (24 vs 12). Intuitively, the fact that the racemization of tetrarosette assembly *P*-**2d**$_3$·(BuCYA)$_{12}$ can in fact be measured seems in contradiction with our earlier observation that **2d**$_3$·(BuCYA)$_{12}$ cannot be formed directly from its components **2d** and BuCYA (even in the presence of *R*BAR).[13] This indicates that the kinetic products obtained after mixing

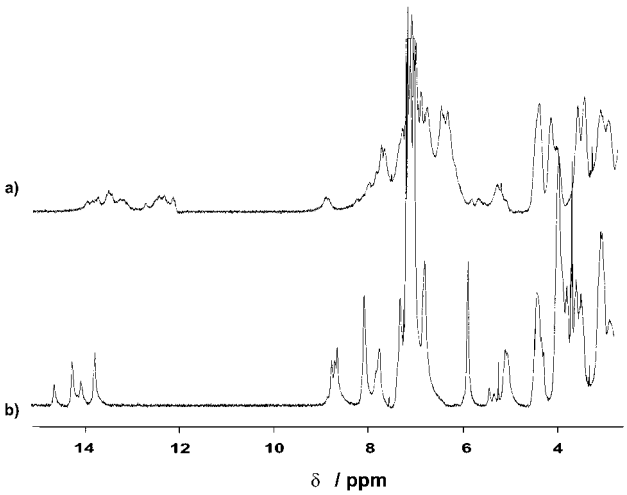

FIGURE 10. (a) ^{1}H NMR spectrum of assembly *P*-**3b**$_3$·(*R*BAR)$_{18}$ in $CDCl_3$ (1.0 mM) at room temperature. (b) ^{1}H NMR spectrum of the same solution after the addition of 1.2 equiv of BuCYA (relative to *R*BAR).

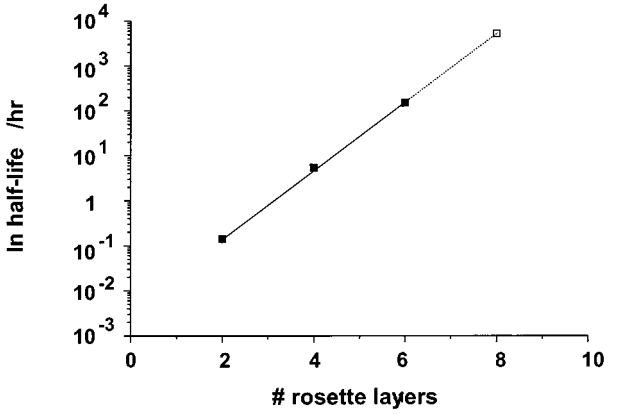

FIGURE 11. Logarithmic plot of the half-life to racemization in chloroform at 50 °C as a function of the number of rosette motifs in the assembly. The half-life to racemization of an octarosette assembly was estimated by extrapolation of the half-lifes of double, tetra-, and hexarosette assemblies.

2d and BuCYA have a much higher kinetic stability than tetrarosette assembly **2d**$_3$·(BuCYA)$_{12}$.

Finally, the racemization of hexarosette assembly *P*-**3b**$_3$·(BuCYA)$_{18}$ was studied. Enantiomerically enriched assembly *P*-**3b**$_3$·(BuCYA)$_{18}$ was prepared in a similar manner as for tetrarosette assembly *P*-**2d**$_3$·(BuCYA)$_{12}$ by adding BuCYA to assembly *P*-**3b**$_3$·(*R*BAR)$_{18}$. The quantitative exchange of *R*BAR for BuCYA was evidenced by the complete disappearance of the numerous signals corresponding to the NH_{RBAR} protons of *P*-**3b**$_3$·(*R*BAR)$_{18}$ and the appearance of only four signals for the NH_{BuCYA} protons of *P*-**3b**$_3$·(BuCYA)$_{18}$ (Figure 10).[27] Subsequently, the racemization of hexarosette assembly *P*-**3b**$_3$·(BuCYA)$_{18}$ was studied under similar conditions as used for the double and tetrarosette assemblies, i.e., in chloroform at 50 °C (Figure 9). These measurements gave a racemization rate constant $k_{rac} = (6.4 \pm 0.5) \times 10^{-7}$ s^{-1} and a corresponding half-life of 150 h (more than 6 days). It should be emphasized that this value is obtained in the presence of *R*BAR, which significantly lowers the half-

life for racemization.[28] Without *R*BAR present, the half-life time would be significantly higher.

The racemization data obtained for the double, tetra- and hexarosette assemblies are summarized in a logarithmic plot of the half-life as a function of the number of rosette layers present in the assemblies. Extrapolation of these data to the next assembly generation, i.e., an assembly comprised of eight rosette layers held together by 144 H-bonds, results in a predicted half-life to racemization of more than 200 days in chloroform at 50 °C (Figure 11).

Conclusions

Chiral amplification experiments with a series of double (36 H-bonds), tetra- (72 H-bonds), and hexarosette (108 H-bonds) assemblies reveal a strong dependence of the kinetic stability of H-bonded assemblies on solvent and temperature. Activation energies of 98.7 ± 16.6 kJ mol^{-1} and 172.8 ± 11.3 kJ mol^{-1} were determined for the dissociation of a tetramelamine from a tetrarosette assembly in chloroform and benzene, respectively. Furthermore, a series of racemization experiments with these assemblies showed that the kinetic stability of H-bonded assemblies is more strongly affected by the number and strength of the H-bonds involved. The racemization half-lifes (in the presence of barbiturate *R*BAR) were found to be 8.4 min, 5.5 h, and 150 h in chloroform at 50 °C, which approaches the racemization half-life times of covalent molecules.

Experimental Section

THF was freshly distilled from Na/benzophenone, EtOAc and hexane (referring to petroleum ether fraction with bp 60−80 °C) from K_2CO_3, and CH_2Cl_2 from $CaCl_2$. All chemicals were of reagent grade and used without further purification. Residual solvent protons were used as internal standard for NMR spectra and chemical shifts are given relative to tetramethylsilane (TMS). CD and UV/vis spectra were recorded at room temperature. FAB-MS spectra were recorded with *m*-nitrobenzyl alcohol (NBA) as a matrix. EI mass spectra were recorded with an ionizing voltage of 70 eV. MALDI TOF measurements were performed on a mass spectrometer equipped with delayed extraction. A UV nitrogen laser (λ = 337 nm) which produced 3 ns pulses was used, and the mass spectra were obtained both in the linear and reflectron mode. Mass assignments were performed with nonmanipulated spectra (no smoothing or centering, etc.). The presence of solvents in the analytical samples was confirmed by ^{1}H NMR spectroscopy. Flash column chromatography was performed using silica gel (SiO_2, E. Merck, 0.040−0.063 mm, 230−240 mesh). All reagents were commercially obtained and used without further purification.

The synthetic procedures for calix[4]arene dimelamines **1a**−**c** and **4a**,[16] **1d**,[29] **8**,[31] *R*BAR,[25] and BuCYA[16] have been published elsewhere.

5-*N*-[4-Amino-6-(3-amino-2,2-dimethylpropylamino)-1,3,5-triazin-2-yl]amino-17-*N*-[4-amino-6-(3-N-Boc-amino-2,2-dimethyl-1,3-propylamino)-1,3,5-triazin-2-yl]amino-25,26,27,28-tetrapropoxycalix[4]arene (1e). A solution of 99% di-*tert*-butyl dicarbonate (0.237 g, 1.08 mmol) in THF was added dropwise over 30 min to a solution of **8**[31] (1.0 g, 0. 98 mmol) and DIPEA (0.189 mL, 1.08 mmol) in THF. The reaction mixture was stirred for an additional 60 min and then evaporated to dryness. The residue was redissolved in CH_2Cl_2, washed with NaOH (1 N), H_2O, and brine, and dried over Na_2SO_4. After evaporation of the solvent, the residue was purified by flash column chromatography (SiO_2, 9/1 CH_2Cl_2/CH_3OH−1% NH_4OH) giving **1e** as a white solid (360 mg, 33%). ^{1}H NMR: δ = 7.1−6.7 (br m, 6H), 6.6−6.1 (br m, 4H), 5.6−4.6 (br m, 6H), 4.38 and 3.09 (ABq, 8H, ^2J(H,H) = 13.4 Hz), 3.9−4.0 (m, 4H), 3.55−3.65 (m, 4H), 3.2 (br s, 4H), 2.8 (br s), 2.4 (br s, 2H), 2.0−1.8 (m, 8H), 1.43 (s, 9H), 1.05 (t, 6H, ^3J(H,H) = 7.4 Hz), 0.84 (m, 18H). MS (FAB): *m*/*z* = 1111.7 (100) ([M + H^+], calcd 1110.7). Anal. Calcd for $C_{61}H_{86}O_6N_{14}$: calcd C 65.92, H 7.80, N 17.64; found: C 65.38, H 7.72, N 17.70.

Tetramelamine 2d. To a solution of monoBoc-protected dimelamine **1e** (113 mg, 0.1 mmol) and DIPEA (19 mL, 0.11 mmol) in CH_2Cl_2 was added instantaneously a solution of 1,4-butyl-bis(*p*-nitrophenyl) dicarbamate (21 mg, 0.05 mmol) in CH_2Cl_2, and the reaction was stirred overnight at rt. Subsequently, the reaction mixture was washed with aqueous NaOH (1 N), H_2O, and brine and dried over Na_2SO_4. After removal of the solvent under reduced pressure, the residue was purified by flash column chromatography (SiO_2, CH_2Cl_2/CH_3OH−1%NH_4OH, 90:10) affording **2d** as a white solid (114 mg, 95%). ^{1}H NMR: δ = 7.2−6.6 (br m, 12H), 6.6−5.9 (br m, 12H), 5.8−4.8 (br m, 12H), 4.39 and 3.12 (ABq, 16H, ^2J(H,H) = 13.4 Hz), 4.0−3.9 (m, 8H), 3.6 (m, 8H), 3.2 (br s, 8H), 2.8 (br s 8H), 2.7−2.6 (br s, 4H), 2.0−1.8 (m, 20H), 1.43 (s, 18H), 1.05 (t, 12H, ^3J(H,H) = 7.4 Hz), 0.9 (m, 36H). MS (FAB): *m*/*z* = 2361.4 (100, M^+, calcd 2361.3). Anal. Calcd for $C_{128}H_{180}N_{30}O_{14}$·$5CH_3OH$: C 62.99, H 8.05, N 16.44; found: C 62.77, H 7.38, N 16.30.

5-*N*-[4-amino-6-(3-(4-*N*-(*p*-nitrophenoxycarbonylamino)-butylureido)-2,2-dimethylpropylamino)-1,3,5-triazin-2-yl]amino-17-*N*-[4-amino-6-(3-(*t*-BOC-amino)-2,2-dimethylpropylamino)-1,3,5-triazin-2-yl]amino-25,26,27,28-tetrapropoxycalix[4]arene (1f). To a refluxing solution of 1,4-butyl-bis(*p*-nitrophenyl) dicarbamate (0.885 g, 2.11 mmol) in acetone (300 mL) was added a solution of N-Boc-protected dimelamine **1e** (0.235 g, 0.21 mmol) and DIPEA (40 μL, 0.23 mmol) in CH_2Cl_2 (20 mL). The reaction mixture was refluxed overnight, the solvent was evaporated, and the product was extracted from the residue (excess of dicarbamate) with CH_2Cl_2. Crude **1f** was further purified by column chromatography (SiO_2, CH_2Cl_2/CH_3OH, 96:4) giving **1f** as a white powder in 71% yield (208 mg, 0.15 mmol). ^{1}H NMR: δ = 8.12 (d, 2H, ^{3}J(H,H) = 8.7 Hz), 7.22 (d, 2H, ^{3}J(H,H) = 8.7 Hz), 7.1−6.7 (br m, 6H), 6.6−6.1 (br m, 4H), 5.6−4.6 (br m, 6H), 4.38 and 3.11 (ABq, 8H, ^2J(H,H) = 13.4 Hz), 4.0−3.9 (m, 4H), 3.65−3.55 (m, 4H), 3.2 (m, 4H), 3.0−2.8 (m, 4H), 2.0−1.8 (m, 8H), 1.43 (s, 9H), 1.05 (t, 6H, ^3J(H,H) = 7.4 Hz), 0.84 (m, 18H). MS (FAB): *m*/*z* = 1390.8 (100, M^+, calcd for $C_{73}H_{99}O_{11}N_{17}$: 1390.7). A satisfactory elemental analysis of this product could not be obtained.

Hexamelamine 3b. To a solution of monoBoc dimelamine **1f** (0.230 g, 0.165 mmol) and DIPEA (28 μL, 0.16 mmol) in CH_2Cl_2 (10 mL) was added dimelamine **8** (84 mg, 0.083 mmol), and the solution was stirred overnight at rt. Subsequently, the solution was washed with $NaHCO_3$ (1 N), H_2O, brine and dried over Na_2SO_4. The product was evaporated to dryness and further purified by flash column chromatography (SiO_2, CH_2Cl_2/CH_3OH−1%NH_4OH, 90:10) to give pure hexamelamine **3b** as a white solid in 85% yield (0.246 g, 0.070 mmol). ^{1}H NMR: δ = 7.2−6.6 (br m, 18H), 6.6−5.9 (br m, 18H), 5.6−4.6 (br m, 18H), 4.38 and 3.07 (ABq, 24H, ^2J(H,H) = 13.4 Hz), 4.0−3.9 (m, 12H), 3.7 (br s, 12H), 3.55 (m, 12H), 2.8 (br s, 8H), 2.7−2.6 (br s, 4H), 2.0−1.8 (m, 32H), 1.4 (s, 18H), 1.05 (t, 18H, ^{3}J(H,H) = 7.4 Hz), 0.9 (m, 54H). MS (FAB): *m*/*z* = 3513.6 (100, [M + H]$^+$, calcd 3512.1). Anal. Calcd for $C_{190}H_{266}N_{46}O_{20}$·$2H_2O$: calcd C 64.27, H 7.66, N 18.15; found: C 64.39, H 7.44, N 17.74.

5-*N*-[4-Amino-6-(*S*)-1-phenylethylamino-1,3,5-triazin-2-yl]amino-17-amino-25,26,27,28-tetrapropoxycalix[4]-arene (4b). Compound **4b** was obtained as an off-white solid (99%) following the procedure described for the enantiomer **4a**.[16] Both compounds have identical ^{1}H NMR spectra. MS

(31) Kerckhoffs, J. M. C. A.; Crego-Calama, M.; Luyten, I.; Timmerman, P.; Reinhoudt, D. N. *Org. Lett.* **2000**, *2*, 4121−4124.

(FAB): *m*/*z* 837.2 ([M + H]$^+$, calcd 837.1). Anal. Calcd for $C_{51}H_{61}O_4N_7 \cdot 0.2H_2O$: C 72.95, H 7.37, N 11.68; found C 72.97, H 7.23, N 11.28.

5-*N*-[4-Amino-6-(*R*)-1-phenylethylamino-1,3,5-triazin-2-yl]amino-17-*N*-[4-amino-6-(3-(aminomethyl)phenylmethylamino)-1,3,5-triazin-2-yl]amino-25,26,27,28-tetrapropoxycalix[4]arene (5a). To an ice-cold solution of **4a** (0.72 g, 0.86 mmol) and DIPEA (0.37 mL, 2.15 mmol) in THF (40 mL) was added cyanuric chloride (0.17 g, 0.95 mmol), and the solution was stirred for 3 h at 0 °C. A stream of ammonia gas was then bubbled through the solution for a period of 2 h, while the temperature was maintained at 0 °C. The solvent was removed under reduced pressure, and the residue was partitioned between CH_2Cl_2 and H_2O. The organic layer was washed with H_2O and brine, dried ($MgSO_4$), and the solvent was removed under reduced pressure. The resulting intermediate compound **4a^I** was obtained as a white solid and used without further purification or analysis. Compound **4a^I** (0.16 g, 0.17 mmol) was stirred overnight at 70 °C in *m*-xylylenediamine (4.0 mL, 30.3 mmol). After cooling the mixture to room temperature, H_2O (20 mL) was added, and the white precipitate that formed was collected, washed with H_2O, and redissolved in CH_2Cl_2. After drying over Na_2SO_4, the solvent was evaporated under reduced pressure. Purification by flash column chromatography (SiO_2, CH_2Cl_2/MeOH/NH_4OH = 90/9.5/0.5%) gave **5a** as a white solid (0.12 g, 68%). ^{1}H NMR (300 MHz, THF-d_8) δ 8.0−7.0 (m, 15H), 6.5−6.0 (m, 8H), 5.8−5.4 (m, 4H), 5.3 (br s, 1H), 4.57 (d, 2H, $^3J_{NH}$ = 12.1 Hz), 4.43 and 3.06 (ABq, 8H, $^2J_{HH}$ = 13.2 Hz), 4.4 (br s, 2H), 3.94 (br s, 4H), 3.73 (br s, 4H), 2.45 (br s, 2H) 2.10−1.60 (m, 8H), 1.49 (d, 3H, $^3J_{HH}$ = 7.0 Hz), 1.09 (t, 6H, $^3J_{HH}$ = 6.0 Hz), 0.95 (br s, 6H). MS (FAB): *m*/*z* 1064.5 ([M + H]$^+$, calcd 1064.6). Anal. Calcd for $C_{62}H_{73}O_4N_{13}$: calcd C 69.97, N 17.11, H 6.91; found: C 69.98, N 17.01, H 6.91.

5-*N*-[4-Amino-6-(*S*)-1-phenylethylamino-1,3,5-triazin-2-yl]amino-17-*N*-[4-amino-6-(3-(aminomethyl)phenylmethylamino)-1,3,5-triazin-2-yl]amino-25,26,27,28-tetrapropoxycalix[4]arene (5b). Compound **5b** was obtained as a white solid (71%) following the procedure described for compound **5a** starting from **10**. The ^{1}H NMR spectrum of **5b** is identical to that of compound **5a**. MS (FAB): *m*/*z* 1064.6 ([M + H]$^+$, calcd 1064.6). $C_{62}H_{73}O_4N_{13}$: calcd C 69.97, N 17.11, H 6.91; found: C 70.16, N 17.05, H 6.96.

Tetramelamine 2a. A solution of **5a** (0.13 g, 0.12 mmol), **4a^I** (0.12 g, 0.11 mmol), and DIPEA (0.1 mL, 57 mmol) in THF (5 mL) was refluxed for 7 days. The solvent was removed under reduced pressure, and the residue was redissolved in CH_2Cl_2, washed with H_2O and brine, and dried over Na_2SO_4. Evaporation of the solvent under reduced pressure gave compound **2a** (0.15 g, 62%) as a white solid after flash column chromatography (SiO_2, CH_2Cl_2/MeOH/NH_4OH = 92.5/7.0/0.5%). ^{1}H NMR (300 MHz, THF-d_8) δ 7.64 (br s, 4H), 7.4−6.8 (br m, 22H), 6.4−6.0 (br s, 16H), 5.6−5.4 (br s, 8H), 5.21 (br s, 2H), 4.41 (br s, 4H), 4.30 and 2.93 (ABq, 16H, $^2J_{HH}$ = 13.2 Hz), 3.79 (br s, 8H), 3.62 (br s, 8H), 2.0−1.7 (m, 16H), 1.36 (d, 6H, $^3J_{HH}$ = 6.9 Hz), 0.95 (t, 12H, $^3J_{HH}$ = 7.0 Hz), 0.84 (t, 12H, $^3J_{HH}$ = 7.0 Hz). MS (FAB): *m*/*z* 1992.7 ([M + H]$^+$, calcd 1992.1). Anal. Calcd for $C_{116}H_{134}N_{24}O_8 \cdot 2H_2O$: C 68.67, N 16.57, H 6.86; found: C 68.87, N 16.45, H 6.62.

Tetramelamine 2b. Compound **2b** was obtained as an off-white solid (82%) following the procedure described for compound **2a**. The ^{1}H NMR spectrum of **2b** is identical to that of compound **2a**. MS (FAB): *m*/*z* 1992.4 ([M + H]$^+$, calcd 1992.1). Anal. Calcd for $C_{116}H_{134}N_{24}O_8$: C 69.93, N 16.87, H 6.78; found: C 69.76, N 16.57, H 6.68.

5-*N*-[4-Amino-6-(*R*)-1-phenylethylamino-1,3,5-triazin-2-yl]amino-17-*N*-[4-amino-6-(3-amino-2,2-dimethylpropylamino)-1,3,5-triazin-2-yl]amino-25,26,27,28-tetrapropoxycalix[4]arene (6). Compound **6** was obtained as a white solid (87%) following a similar procedure as described for compound **5a**. ^{1}H NMR (300 MHz, $CDCl_3$) δ 7.4−7.3 (m, 6H), 7.0−6.8 (m, 7H), 6.4−6.2 (m, 6H), 5.3−5.0 (m, 7H), 4.44 and 3.13 (ABq, 8H, $^2J_{HH}$ = 12.8 Hz), 4.00 and 3.71 (2 br s, 8H), 3.21 (s, 2H), 2.44 (s, 2H), 2.0−1.8 (m, 8H), 1.53 (d, 3H, $^3J_{HH}$ = 5.4 Hz), 1.09 (t, 6H, $^3J_{HH}$ = 7.2 Hz), 1.0−0.9 (m, 12H). MS (FAB): *m*/*z* 1030.5 ([M + H]$^+$, calcd 1030.6). No satisfactory elemental analysis of this compound could be obtained.

Tetramelamine 2c. To a refluxing solution of 1,4-diaminobutane bis(*p*-nitrophenyl) dicarbamate[13] (0.08 g, 0.19 mmol) in acetone (50 mL) was added a solution of **6** (0.40 g, 0.38 mmol) and DIPEA (68 μL, 0.38 mmol) in CH_2Cl_2 (10 mL). The reaction mixture was refluxed overnight, after which the solvent was evaporated. Purification using flash column chromatography (SiO_2, CH_2Cl_2/CH_3OH = 92/8) gave **2c** as a white solid (0.35 g, 41%). ^{1}H NMR (300 MHz, THF-d_8) δ 7.8 (br s, 4H), 7.4−7.1 (m, 18H), 6.5−6.3 (m, 16H), 6.1−6.0 (br s, 4H), 5.7 (br s, 6H), 5.4−5.3 (br s, 4H), 4.43 and 3.12 (ABq, 16H, $^2J_{HH}$ = 12.8 Hz), 3.93 and 3.74 (2 br s, 16H), 3.2−3.1 (m, 8H) 2.96 (s, 4H), 2.0−1.9 (m, 16H), 1.5−1.4 (br s, 10H), 1.09 and 0.96 (2 t, $^3J_{HH}$ = 7.2 Hz, 24H), 0.86 (s, 12H). MS (FAB): *m*/*z* 2201.2 ([M + H]$^+$, calcd 2201.3). Anal. Calcd for $C_{124}H_{158}N_{28}O_{10} \cdot H_2O$: C 67.12, N 17.68, H 7.27; found: C 67.10, N 17.42, H 7.14.

5-*N*-[4-Amino-6-(*R*)-1-phenylethylamino-1,3,5-triazin-2-yl]amino-17-*N*-[4-amino-6-(3-(4-*N*-(*p*-nitrophenoxycarbonylamino)butylureido)-2,2-dimethylpropylamino)-1,3,5-triazin-2-yl]amino-25,26,27,28-tetrapropoxycalix[4]arene (7). To a refluxing solution of 1,4-diaminobutane bis(*p*-nitrophenyl) dicarbamate[13] (1.0 g, 2.4 mmol) in acetone (300 mL) was added a solution of **6** (0.25 g, 0.24 mmol) and DIPEA (46 μL, 0.26 mmol) in CH_2Cl_2 (20 mL). The reaction mixture was refluxed overnight, after which the solvent was evaporated. The product was extracted from the residue (excess of dicarbamate) with CH_2Cl_2. Subsequently, purification using flash column chromatography (SiO_2, CH_2Cl_2/CH_3OH = 92/8) gave **7** as a white solid (120 mg, 42%). ^{1}H NMR (300 MHz, $CDCl_3$) δ 8.23 (d, 2H, $^3J_{HH}$ = 8.4 Hz), 7.3−7.2 (m, 7H), 7.1−6.8 (m, 6H), 6.5−6.2 (m, 6H), 5.95 (s, 1H), 5.62 (s, 1H), 5.3−4.8 (br m, 6H), 4.45 and 3.12 (ABq, 8H, $^2J_{HH}$ = 12.8 Hz), 4.04 and 3.68 (2 br s, 8H), 3.3−3.2 (m, 6H), 2.88 (s, 2H), 2.0−1.8 (m, 8H), 1.5 (br s, 7H), 1.09 (t, 6H, $^3J_{HH}$ = 7.2 Hz), 0.9 (m, 12H). MS (FAB): *m*/*z* 1171.7 ([M − $C_6H_4NO_2$ + H]$^+$, calcd 1170.6). No satisfactory elemental analysis of this compound could be obtained.

Hexamelamine 3a. A mixture of **7** (100 mg, 0.08 mmol), **8**[31] (38 mg, 0.038 mmol), and DIPEA (7.2 μL, 0.041 mmol) in CH_2Cl_2 (15 mL) was refluxed overnight. After evaporation of the solvent, compound **3a** was obtained after flash column chromatography (SiO_2, CH_2Cl_2/CH_3OH = 92/8) as a white solid (115 mg, 79%). ^{1}H NMR (300 MHz, THF-d_8) δ 7.8 (br s, 6H), 7.3−7.0 (m, 26H), 6.5−6.0 (m, 28H), 5.7 (br s, 8H), 5.3 (br s, 6H), 4.41 and 3.14 (ABq, 24H, $^2J_{HH}$ = 12.8 Hz), 3.92 and 3.75 (2 br s, 24H), 3.2−3.1 (m, 16H), 2.96 (s, 8H), 2.0−1.9 (m, 24H), 1.5−1.4 (br s, 14H), 1.09 and 0.96 (2 t, $^3J_{HH}$ = 7.2 Hz), 0.86 (s, 24H). MS (FAB): *m*/*z* 3352.1 ([M + H]$^+$, calcd 3350.9). Anal. Calcd for $C_{186}H_{244}N_{44}O_{16}$: C 66.64, N 18.38, H 7.34; found: C 66.84, N 18.39, H 7.51.

JO0201023